Phase Coherence in the Inelastic Cotunneling Regime

Martin Sigrist,[1] Thomas Ihn,[1] Klaus Ensslin,[1] Daniel Loss,[2] Matthias Reinwald,[3] and Werner Wegscheider[3]
[1]*Solid State Physics Laboratory, ETH Zürich, 8093 Zürich, Switzerland*
[2]*Department of Physics and Astronomy, University of Basel, Klingelbergstrasse 82, CH-4056 Basel, Switzerland*
[3]*Institut für experimentelle und angewandte Physik, Universität Regensburg, Germany*
(Received 23 June 2005; published 26 January 2006)

Two quantum dots with tunable mutual tunnel coupling have been embedded in a two-terminal Aharonov-Bohm geometry. Aharonov-Bohm oscillations investigated in the cotunneling regime demonstrate coherent tunneling through nonresonant states. Visibilities of more than 0.8 are measured indicating that phase-coherent processes are involved in the elastic and inelastic cotunneling. An oscillation-phase change of π is detected as a function of bias voltage at the inelastic cotunneling onset.

DOI: 10.1103/PhysRevLett.96.036804 PACS numbers: 73.23.Hk, 03.65.−w, 73.40.Gk, 73.63.Kv

Is electron transport through quantum dots phase coherent? This question roots in the discussion of how to describe it: by incoherent sequential tunneling, or by coherent resonant tunneling? The observation of interference effects have proven that the current through quantum dots (QDs) has phase-coherent contributions [1–4]. In pioneering experiments Aharonov-Bohm (AB) oscillations were detected on conductance resonances of a dot embedded in an AB interferometer [1]. A QD molecule with source and drain contacts common to both dots has been reported to exhibit AB oscillations when the tunnel coupling between the dots is negligible [2]. Phase-coherent transport through QDs allowed the observation of the Fano effect in a ring [3] and the Kondo effect in QDs [4]. Proposals exist to use QDs as qubits [5] and to probe the entanglement of singlet and triplet states by their distinct AB phases [6]. Theoreticians discuss how far interactions in QDs dephase the transmitted electrons [7,8].

We report measurements tackling the question of the coherence of elastic and inelastic cotunneling through QDs [9,10]. Decoherence is generated by which-path detection [11]. Inelastic processes are generally believed to lead to decoherence. An inelastic cotunneling path cannot interfere with an alternative elastic cotunneling path because the former leaves the QD in an excited state, thus leaving a trace as to which path the electron took. We demonstrate experimentally a situation in which elastic and inelastic cotunneling processes coexist with phase-coherent AB oscillations. This means that inelastic cotunneling processes that do not allow which-path detection are not detrimental for the phase-coherence. Our interferometer structure consists of a QD molecule embedded in an AB ring, similar to Ref. [2], thus realizing systems considered theoretically [6–8,12].

The sample shown in Fig. 1(a) is based on a Ga[Al]As heterostructure with a two-dimensional electron gas (2DEG) 34 nm below the surface. It was fabricated by multiple layer local oxidation with a scanning force microscope (SFM) [13]: The 2DEG is depleted below the oxide lines written on the GaAs cap layer. A thin Titanium film is then evaporated on top and cut by local oxidation into mutually isolated parts acting as top gates.

The resulting AB interferometer [Fig. 1(a)] has a source and drain opening transmitting at least one mode and being tunable by the top gates sd1 and sd2. One QD is embedded in each arm of the ring. The two dots are tunnel coupled via a quantum point contact (QPC) which constitutes an internal connection between the two branches of the ring. The

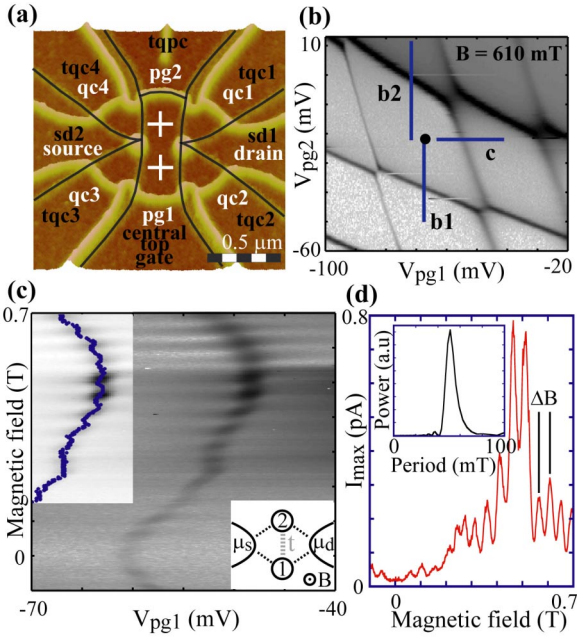

FIG. 1 (color online). (a) SFM micrograph of the structure. In-plane gates (white letters), Titanium oxide lines (black lines), and top gates (black letters) are indicated. The QDs are marked by white crosses. (b) Charge stability diagram of the double QD. (c) Conductance peak of dot 1 as a function of magnetic field and gate pg1 [corresponding to the horizontal line c in (b)]. Upper inset: the same peak with a line indicating its maximum. Lower inset: schematic of the double QD embedded in the AB ring. (d) Conductance peak maximum as a function of magnetic field. The AB period is about 50 mT. Inset: Fourier analysis.

strength t of this coupling can be tuned with the central top gate from the tunneling to the open regime. The two oxide dots forming this constriction by depleting the 2DEG will be referred to as ''antidots'' below. Each QD is coupled to the ring by two QPCs tunable via the top gates tqc1-4. The in-plane gates pg1 and pg2 are used as plunger gates for dot 1 and dot 2, respectively. Topologically the sample is similar to those of Refs. [2,14].

The conductance was measured in a two-terminal setup at 80 mK electronic temperature. For weak interdot coupling with the dots strongly coupled to the ring the conductance shows an AB period of 22 mT with a visibility (i.e., the ratio of the AB oscillation amplitude and the magnetic field averaged current) up to 0.2 consistent with interference around the entire ring. With negative voltages applied to tqc1-4 the dots can be tuned into the Coulomb-blockade regime. Each dot has a charging energy of 0.7 meV. In our shallow, top-gated structures it is strongly reduced by image charges in the top gates. Based on the model calculation in Ref. [15] we find a dot radius of 66 nm, only slightly larger than in Ref. [2]. The estimated number of electrons in each dot is about 30. Single-particle level spacings of 0.1 meV are found from nonlinear transport measurements.

In Fig. 1(b) the charge stability diagram of the double dot is shown with a magnetic field of 610 mT applied normal to the 2DEG. It shows the hexagon pattern formed by regions of constant charge in the two dots [16,17]. The 9th root of the conductance is plotted, enhancing the visibility of the small cotunneling current. We use this nonlinear scale for all grayscale figures, except Fig. 3(b). From Fig. 1(b) the capacitive interdot coupling is estimated to be a tenth of the intradot charging energy and twice the thermal smearing of conductance resonances.

In Fig. 1(c) we demonstrate that the field scales for energy-level crossings in the QDs (i.e., fluctuations of the conductance peak positions with magnetic field) and for the AB effect are well separated. A conductance peak of dot 1 was measured as a function of V_{pg1} and magnetic field while keeping dot 2 off-resonance along line ''c'' in Fig. 1(b). The peak shifts smoothly on the scale of a few hundred mT (about one flux quantum through the dot). The peak amplitude oscillates on a smaller scale with a period $\Delta B \approx 50$ mT.

In Fig. 1(d) we show the height of the conductance peak as a function of magnetic field extracted from this measurement [upper inset of Fig. 1(c)] and its Fourier transform. The period ΔB of the oscillations corresponds to an area of 165 nm radius, i.e., to interference paths encircling only one of the two antidots. The oscillations indicate phase-coherent transmission through both QDs. The oscillation amplitude is a significant fraction (up to 0.5) of the total current showing that the phase-coherent contribution to the total current is also significant. Visibilities of up to 0.8 were observed on resonances of dot 1 in some parameter regions. This is a remarkable number if compared to the visibilities observed in other experiments (e.g., [2]). AB oscillations with dot 2 on and dot 1 off resonance were similar, but had a smaller visibility.

Only dot 1 is on resonance in Fig. 1(d) while dot 2 allows an elastic cotunneling current. No AB effect was observed in this regime in Ref. [2]. Figure 1(c) shows that in our experiment AB oscillations are even observed when both dots are in the elastic cotunneling regime, far away from conductance peaks. In such regions the visibility can take values of more than 0.8 in this sample.

We proceed by identifying the inelastic cotunneling onset in one of the QDs from the Coulomb-blockade diamonds shown in Fig. 2. Figure 2(a) shows the differential conductance as a function of V_{bias} taken at a magnetic field of 630 mT in the center of a hexagon as indicated by the black dot in Fig. 1(b). A current step found for positive V_{bias} indicates the onset of inelastic cotunneling [10]. Coulomb diamonds for dot 2 [Fig. 2(b)] measured along the lines ''b1'' and ''b2'' [Fig. 1(b)] show the typical situation observed in single dots: the inelastic onset depends on the number of electrons on dot 2 and is related to excited states outside the Coulomb-blockaded region [10]. For dot 1 [Fig. 2(c)] measured along line c in Fig. 1(b), a superposition of Coulomb diamonds and an inelastic cotunneling onset in the current is observed. The inelastic onset is not affected, if an electron is added to dot 1. We conclude that depending on bias voltage, the current through dot 2 is dominated either by elastic or inelastic cotunneling while the current through dot 1 involves elastic cotunneling only.

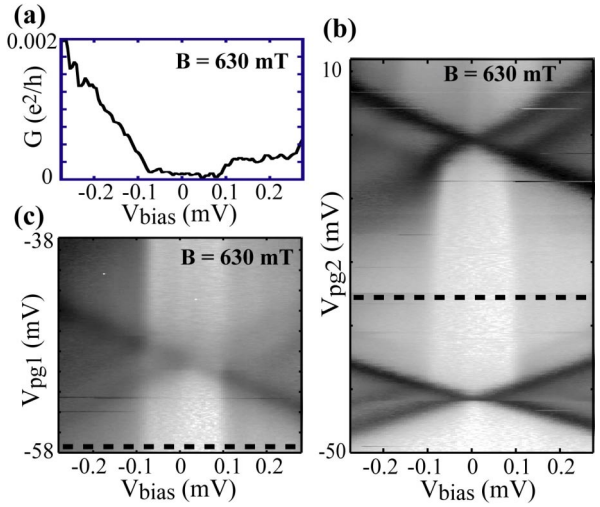

FIG. 2 (color online). (a) Differential conductance measured as a function of V_{bias} [in-plane gates fixed at black dot in Fig. 1(b)]. This curve is indicated in (b) and (c) and in Fig. 3(a) as a dashed line. (b) Differential conductance measured along lines b1 and b2 in Fig. 1(b) as a function of V_{bias} and V_{pg2}. (c) Differential conductance measured along line c in Fig. 1(b) as a function of V_{bias} and V_{pg1}.

As a next step we investigate the phase coherence of the elastic and inelastic processes. We explore the magnetic field dependence of the inelastic cotunneling onset and look for AB oscillations. Both dots are kept in the cotunneling regime with the in-plane gates fixed [black dot in Fig. 1(b)]. The differential conductance as a function of magnetic field and V_{bias} is shown in Fig. 3(a). Two inelastic cotunneling onsets (marked by arrows) are observed, both depending strongly on magnetic field. Faint vertical stripes with the period of interference around one antidot indicate the presence of AB oscillations across the top right inelastic onset in Fig. 3(a).

The inelastic onset in the black rectangle measured with higher resolution is plotted in Fig. 3(b). The AB oscillations in the elastic cotunneling regime for small V_{bias} are faint and gradually disappear with increasing voltage. At the onset of inelastic cotunneling strong AB oscillations appear, indicating that the inelastic process does not impair phase coherence.

Cross sections through the data in Fig. 3(b) taken along the dashed lines are depicted in Fig. 3(c). The phase of the AB oscillations changes by π when we cross the inelastic cotunneling onset, as already evident in the grayscale plot of Fig. 3(b). At the same time the AB amplitude increases by a factor of 2 and the field averaged (background) conductance increases by a factor of 4. All these changes are well above experimental error. They confirm that at the inelastic cotunneling onset there is a new transport channel taking over in the coherent transport through dot 2. The visibility, in particular, in the elastic cotunneling regime, is exceptionally high indicating that dephasing along the interfering paths is very weak. We attribute the slight increase of the background current (averaging the oscillations) to the magnetic field dependence of the involved energy levels in the dot.

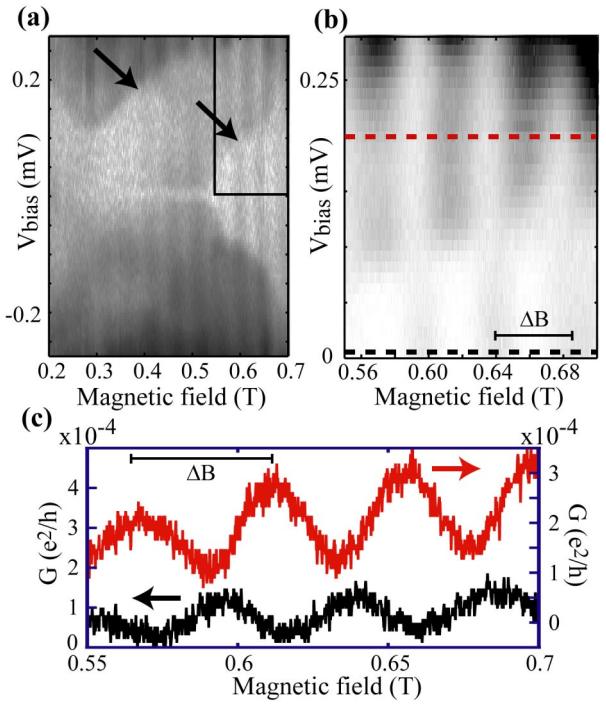

FIG. 3 (color online). (a) Differential conductance as a function of magnetic field and V_{bias} with both dots in the cotunneling regime. (b) Detail of (a) inside the black rectangle. The grayscale is linear. (c) Two traces for small (left axis) and high bias voltage (right axis) are extracted from Fig. 3(b), as indicated by dashed lines.

Similar AB oscillations were also found in neighboring hexagons. The oscillation amplitude depends on the position in the hexagon, being weakest at the hexagon center and increasing towards the boundaries, consistent with standard cotunneling models [9].

Similar measurements performed in the regime of weaker tunnel coupling between the QDs exhibit AB oscillations with a period of 22 mT. The period corresponds to interfering paths encircling both antidots, i.e., to the whole ring area. In this regime, the oscillations were only observed in the inelastic cotunneling regime (visibility about 0.05), because the elastic cotunneling current was smaller than our current-noise level of about 5 fA.

The observed AB period corresponds to paths around one antidot [Fig. 4(a)]. For the discussion we choose to describe the electron transfer through the system as a two-step process: (1) the system goes from its initial state to a virtual intermediate state [e.g., step 1 in Fig. 4(b) where an electron leaves dot 2], and (2) the system goes from this virtual intermediate state to its final state [e.g., processes 2 in Fig. 4(b)]. Step 2 may have contributions from different paths enclosing an AB flux, as shown in Fig. 4(a), leading to the observed AB period. Our experiment proves only coherence between paths contributing to step 2. Because both dots are in the cotunneling regime this implies interference between the non-energy-conserving direct path 2' and the alternative two-step process 2a, 2b which involves an additional virtual state in dot 1. The processes described above and shown in Fig. 4 are one set out of several that would lead to the observed interference, but based on our measurements we consider it to be one of the most likely scenarios. In any case, the concerted tunneling of more than one electron in the sense of cotunneling will be involved and this fact is not detrimental for the observation of interference.

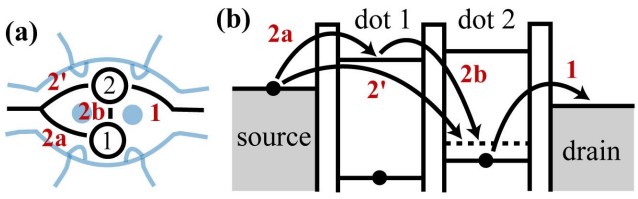

FIG. 4 (color online). (a) Example for a pair of possible interfering paths in the AB interferometer. (b) The same interfering paths in the energy-level diagram.

We interpret the phase change between elastic and inelastic cotunneling observed in Fig. 3(c) as the fingerprint of the excited state in dot 2. The relative phase of the propagating electron between its entrance and exit point contacts depends on the wave function involved. Our measurement shows that there is a phase change of π when the state involved in transport changes from the ground to the excited state. The value of π is compatible with the phase rigidity expected for a two-terminal measurement and to a possible phase difference of π in the tunnel coupling matrix elements of the ground and the excited state in dot 2.

The huge numbers found for the visibilities in our experiment are remarkable. We argue that the involved cotunneling processes require a short tunneling time of the order of $h/U \sim 10$ ps (U is half the charging energy) which is short compared to dephasing times of more than 1 ns reported in other experiments [1]. Perhaps even higher order cotunneling processes than those mentioned above as examples can take place.

Why do we measure no significant suppression of the AB interference by inelastic cotunneling? Considering the data, the most likely explanation is that exemplified in Fig. 4 where the excited state in dot 2 does not allow which-path detection. This is conceivable, if the two interfering paths both start in the source contact and end in dot 2, one taking the detour via dot 1.

Another possible scenario would require that the excited state extends into both dots and therefore does not allow which-path detection [6]. Our experiment is a significant step toward this proposed detection of entanglement via the AB effect [6]. Beyond the demonstration of coherence in the elastic and inelastic cotunneling regime we have chosen the hexagon investigated above in such a way that it is bounded by states which move in a fashion highly correlated with magnetic field. Such states are commonly believed to be spin pairs [18], i.e., states of different spin but with the same orbital wave function. We therefore speculate that in each dot one unpaired spin occupies the highest orbital level. However, the exchange coupling necessary for the formation of singlet and triplet states was probably too low in our experiment due to the moderate tunnel coupling between the dots.

In conclusion, we have experimentally demonstrated phase-coherent processes in the elastic and inelastic cotunneling regimes in quantum dots. Visibilities of more than 0.8 were measured indicating that the phase-coherent current dominates the conductance. A phase jump of π was detected at the onset of inelastic cotunneling processes. We anticipate that cotunneling processes could be employed in applications where a huge degree of phase coherence is crucial.

We thank R. Schleser for valuable discussions. Financial support by the NCCR Nanoscience through the Swiss Science Foundation (Schweizerischer Nationalfonds) is gratefully acknowledged.

[1] A. Yacoby, M. Heiblum, D. Mahalu, and H. Shtrikman, Phys. Rev. Lett. **74**, 4047 (1995); E. Buks, R. Schuster, M. Heiblum, D. Mahalu, and V. Umansky, Nature (London) **391**, 871 (1998); M. Sigrist *et al.*, Phys. Rev. Lett. **93**, 066802 (2004).

[2] A. W. Holleitner, C. E. Decker, H. Quin, K. Eberl, and R. H. Blick, Phys. Rev. Lett. **87**, 256802 (2001).

[3] K. Kobayashi, H. Aikawa, S. Katsumoto, and Y. Iye, Phys. Rev. Lett. **88**, 256806 (2002).

[4] D. Goldhaber-Gordon, H. Shtrikman, D. Mahalu, D. Abusch-Magder, U. Meirav, and M. A. Kastner, Nature (London) **391**, 156 (1998); W. G. van der Wiel, S. De Franceschi, T. Fujisawa, J. M. Elzerman, S. Tarucha, and L. P. Kouwenhoven, Science **289**, 2105 (2000).

[5] D. Loss and D. P. DiVincenzo, Phys. Rev. A **57**, 120 (1998).

[6] D. Loss and E. V. Sukhorukov, Phys. Rev. Lett. **84**, 1035 (2000).

[7] J. König and Y. Gefen, Phys. Rev. Lett. **86**, 3855 (2001).

[8] Z. Jiang, Q. Sun, X. C. Xie, and Y. Wang, Phys. Rev. Lett. **93**, 076802 (2004); J. König, Y. Gefen, and A. Silva, Phys. Rev. Lett. **94**, 179701 (2005); Z. Jiang, Q. F. Sun, X. C. Xie, and Y. P. Wang, Phys. Rev. Lett. **94**, 179702 (2005).

[9] D. Averin and Y. Nazarov, Phys. Rev. Lett. **65**, 2446 (1990); M. R. Wegewijs and Y. V. Nazarov, cond-mat/0103579; V. N. Golovach and D. Loss, Phys. Rev. B **69**, 245327 (2004).

[10] S. De Franceschi *et al.*, Phys. Rev. Lett. **86**, 878 (2001); R. Schleser *et al.*, Phys. Rev. Lett. **94**, 206805 (2005).

[11] A. Stern, Y. Aharonov, and Y. Imry, Phys. Rev. A **41**, 3436 (1990).

[12] J. König and Y. Gefen, Phys. Rev. B **65**, 045316 (2002), and references therein; B. Kubala and J. König, Phys. Rev. B **67**, 205303 (2003); S. Cho, R. McKenzie, K. Kang, and C. Kim, J. Phys. Condens. Matter **15**, 1147 (2003); M. L. Ladrón de Guevara, F. Claro, and P. Orellana, Phys. Rev. B **67**, 195335 (2003); K. Kang and S. Y. Cho, J. Phys. Condens. Matter **16**, 117 (2004); V. Moldoveanu, M. Tolea, A. Aldea, and B. Tanatar, Phys. Rev. B **71**, 125338 (2005).

[13] A. Fuhrer *et al.*, Superlattices Microstruct. **31**, 19 (2002), and references therein.

[14] T. Hatano *et al.*, Phys. Rev. Lett. **93**, 066806 (2004); M. C. Rogge *et al.*, Appl. Phys. Lett. **83**, 1163 (2003).

[15] T. Ihn, *Electronic Quantum Transport in Mesoscopic Semiconductor Structures*, Springer Tracts in Modern Physics Vol. 192 (Springer Verlag, New York, 2003).

[16] M. Sigrist *et al.*, Appl. Phys. Lett. **85**, 3558 (2004).

[17] F. Hofmann *et al.*, Phys. Rev. B **51**, 13 872 (1995); W. G. van der Wiel *et al.*, Rev. Mod. Phys. **75**, 1 (2003).

[18] S. Lüscher *et al.*, Phys. Rev. Lett. **86**, 2118 (2001).